

# 1 Role of the surface on tether-tether reactions within a signaling cluster

## 1.1 Introduction

Disordered proteins aid many reactions by acting as biological tethers. They may be permanent tethers tying two globular domains together (e.g. linking the SH2 and catalytic domains of Src [? ]) or a domain to a surface (e.g. tethering critical phosphorylation sites to the membrane, as seen in CD3 $\zeta$  and PD-1 [? ? ]). They may also be transient tethers, catching diffusing particles and tethering them to another molecule, i.e. formin [? ? ]. By tethering molecules or surfaces together, disordered domains increase the effective concentration for a reaction. This increases reaction rates by improving the probability of two molecules bumping into each other through restriction of their diffusive domain.

Given that a surface reduces the exploration space of a molecule, it will naturally increase the effective concentration without a tether. However, it will also reduce the accessibility of a molecule by sometimes occluding, for example, an enzymatic domain from reaching its substrate in the correct orientation. Given that the surface has both positive and negative effects on reaction rates, how does being tethered to a surface impact a reaction compared to being tethered to a smaller domain?

This type of interaction arises frequently with clustered reactions, such as dephosphorylation of a membrane tethered disordered domain by a membrane bound phosphatase [? ]. Experimental studies of such reactions are more easily performed on a sparse matrix such as dextran than on a hard surface [? ]. Therefore, it is important to understand the effect tethering to a surface has over tethering to a matrix. We explore how the presence of a surface influences the reach of a tethered domain and the overall effective concentration.

One example of this type of reaction is programmed death 1 (PD-1) interacting with Src homology region 2 domain-containing phosphatase-1 (SHP-1) or SHP-2 to dephosphorylate other tethered molecules. PD-1 is a transmembrane receptor expressed in active T cells. Interaction of the extracellular domain of PD-1 with its ligands, PD-L1 or PD-L2, can act to inhibit T cell proliferation and cytokine production and may induce cell death. Specifically, PD-L1 has been shown to be expressed on almost all tumor cells, causing a decrease in T cell cytotoxicity against the tumor [? ? ]. This inhibitory signal is propagated by SHP-1/SHP-2 binding phosphorylated tyrosines in the PD-1 cytoplasmic domain. While bound to PD-1, SHP-1/SHP-2 can dephosphorylate other activating complexes in the T Cell, for instance, CD3 $\zeta$  or ZAP-70 [? ]. Given that both PD-1 and CD3 $\zeta$  are attached to the cell membrane, the role of the tether and membrane are critical to understanding the details of this reaction.

## 1.2 Model and Methods

We first investigate the effects of a surface on a single tether without a bound ligand in free-space and half-space. We model the tether as a freely-jointed chain and the unbound ligand as an idealized ghost sphere located tangential to a single segment. To explore the effects of a surface on a single tether, we vary the number of segments and the size of the incoming ligand. We calculate quasi-equilibrium statistics for the FJC and unbound ligand in both free-space and half-space. We calculate how often a ligand is able to bind to an oriented sphere tangentially attached to the polymer, where ‘able to bind’ refers to the specified sphere being empty of both other polymer segments and the surface.

We next explore the effects of a surface on three specific tethers: PD-1, PEG-3, and PEG-28. PEG-3 and PEG-28 are tethers created by attaching a single immunoreceptor tyrosine inhibitory motif (ITIM) to a series of PEG linkers. Each tether is modeled as a freely-jointed chain characterized by their lengths as measured in Kuhn lengths. The tethers are made up of PEG linkers and amino acids, each of which contributes approximately 0.3nm to the length. We assume maximal flexibility in our model by assigning a Kuhn length,  $\delta$ , of 0.3nm. The contour lengths of each tether may be approximated as  $N$  Kuhn lengths,

Table 1: Structure and number of simulated segments in each explored tether.

Tether Name	Structure	N
PD-1	(37392 B2) Bio-SRAARGTIGARRTGQPLKEDPSAVPVFSV DYGELDFQWREKTPEPPVPSVPEQTEY*ATIVFPSG	64
PEG-3	Bio-(PEG)3-DLQEVTY*IQLDHH	16
PEG-28	Bio-(PEG)28-DLQEVTY*IQLDHH	41

where  $N$  is the total number of PEG linkers and amino acids (Table 1). Note that we consider the size of biotin to be negligible for our simulation.

We investigate SHP-1 as a ligand bound to a tether. In order to simulate SHP-1 as a simple sphere, we estimate its size using three different assumptions. We first estimate the volume of SHP-1 based on its molecular weight, 67561Da, as listed in UniProt entry P29350, assuming an average protein density of  $1.41\text{g}/\text{cm}^3$  [? ].

$$(67.5 \times 1000\text{Da}) * (1.66 \times 10^{-27}\text{kg} / \text{Da}) * (1000\text{g} / \text{kg}) / (1.41\text{g} / \text{cm}^3) = 79.468 \text{nm}^3.$$

Approximating the phosphatase domain as a sphere, we can estimate a radius:

$$V = \frac{4}{3}\pi r^3$$

$$79.468 \text{nm}^3 = \frac{4}{3}\pi r^3$$

$$r \approx 2.7 \text{nm}$$

For comparison, we also estimate an upper bound on the radius of SHP-1 from PyMol measurements of the SHP-1 structure (PDB 3PS5). Rounding up for measurement error, the longest part of the structure is 86 Å (Fig. 1). From this we calculate a maximum radius of  $4.3\text{nm}$ .

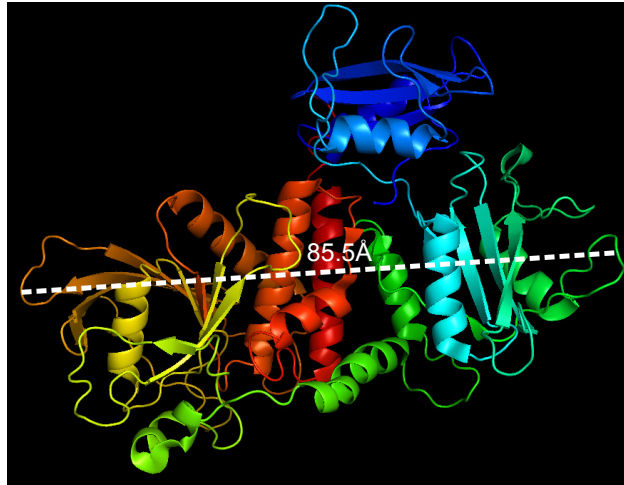


Figure 1: Measurement of maximum length of SHP-1 (PDB 3PS5).

Alternatively, we can estimate the volume of SHP-1 as a rectangular prism and then create a spherical approximation of equal volume. We estimate the length, width and depth of SHP-1 to be 76Å, 36Å, and 58Å respectively, giving a volume of 158688Å<sup>3</sup> (Fig. 2). From this, we calculate the radius for a spherical approximation to be 3.4nm.

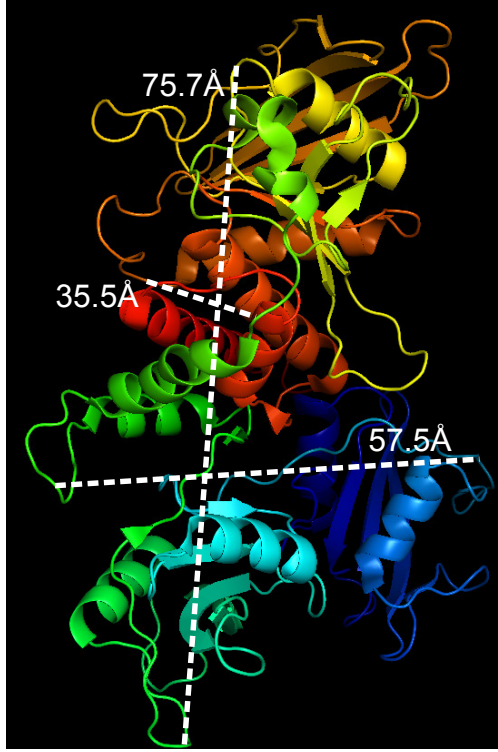


Figure 2: Measurement of rectangular dimensions of SHP-1 (PDB 3PS5).

Using the parameters estimated above, we simulate two equivalent tethers. The idealized SHP1 sphere, or ligand, is bound to the end of one of the tethers. The bound ligand is simulated as an idealized sphere which rotates with the tether. The bound ligand may not occupy the same space as the tether nor may it penetrate the surface if present. The second tether has a ghost ligand attached in the same location (Fig. 3). We allow each tether to explore conformation space, at each conformation determining if the ghost ligand is occluded by the rest of the tether, or in half-space, by the surface. For the tether with the ghost ligand, we record both the location of the center of the ligand and whether or not it was occluded at each conformation. For the tether with the bound ligand, we only record the location. For these simulations, we assume the two tethers are independent and do not sterically influence each other.

We compute the effective concentration as the probability that the bound ligand is near the binding site (where near is defined by within some small radius) and the binding site is not occluded by the rest of the polymer. To calculate this, we separate the tethers from each other by a distance,  $\rho$ , measured in Kuhn lengths by adding  $\rho$  to the  $x$ -coordinate of the ghost ligand. We then measure the distance between the centers of the bound and ghost ligands. If the centers are within a cutoff distance from each other AND the ghost sphere is not occluded, then the bound ligand is able to bind. The effective concentration is calculated by dividing the probability the ligand can bind by the volume of the sphere defined by the cutoff radius.

We fit the effective concentration curves to a half-gaussian curve,  $\sigma_{fit}(\rho) = \sigma_{max} * e^{-\rho^2/l^2}$ , as a function of the separation distance between the two tethers. To fit the simulated data, we use Matlab's `fminsearch` function which uses the Nelder-Mead simplex algorithm. The parameters found by the Nelder-Mead algo-

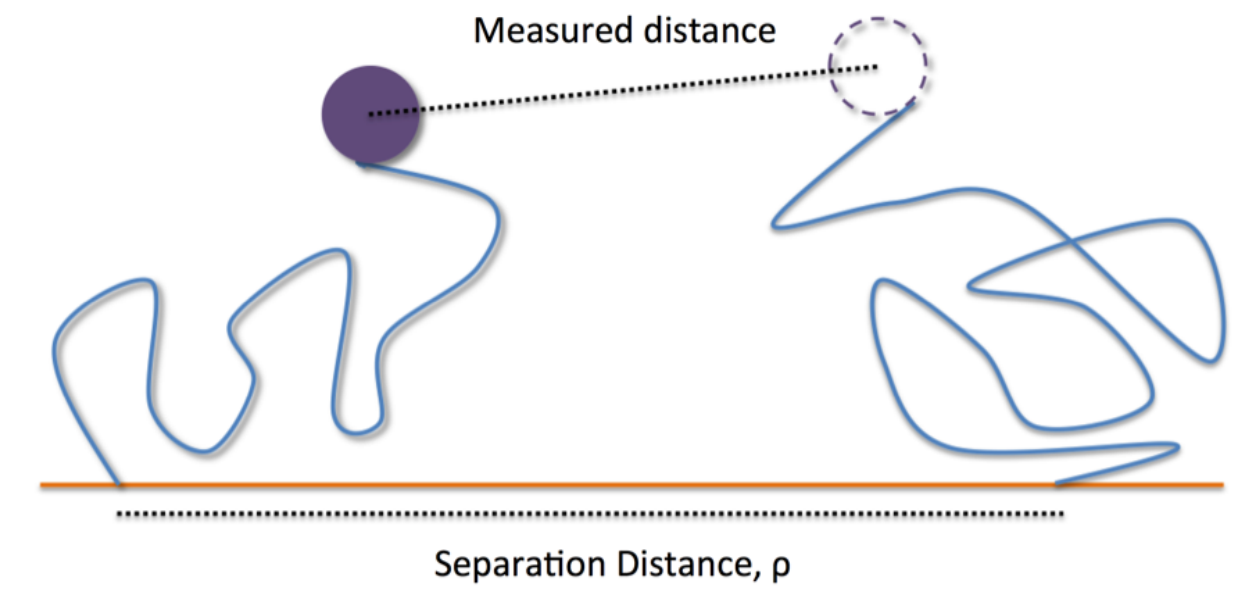


Figure 3: Cartoon of effective concentration simulation in half space.

rithm consistently give a smaller sum of least squares than parameters found using Trust-Region-Reflective Least Squares Algorithm or those found by heuristically sweeping parameter space to minimize the sum of least squares.

## 1.3 Results

### 1.3.1 Accessibility of a reaction site is reduced by the presence of a surface

We first investigate the accessibility of a binding site at the end of the polymer when a surface is present. We record how often the membrane causes the binding site to be inaccessible to its ligand, as opposed to occlusion by the rest of the polymer. We find that occlusion caused only by the membrane increases with the size of the ligand, but decreases with longer polymers (Fig. 4).

We next investigate how the presence of a surface impacts binding of a ligand to a single tether compared to in free-space. We find that a surface consistently net decreases the probability a ligand can bind to a tether, irrespective of tether length or ligand size. For long tethers, the surface reduction is minimal, in some parameters almost eliminating the difference. A larger ligand creates a larger fold decrease in the ability of the kinase to bind in half-space (Fig. 5).

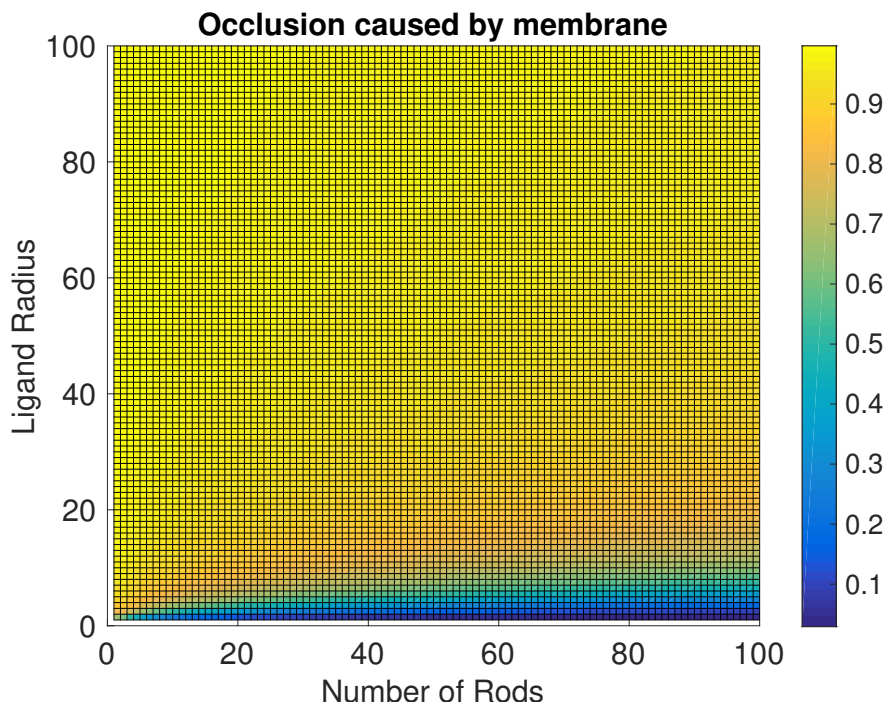


Figure 4: Probability of binding site occlusion due to presence of a surface as a function of polymer length and ligand radius.

### 1.3.2 Future Work: Impact of membrane on reactions between tethered reactants

For a reactant in solution, the reaction rate will be proportional to the concentration of the reactant. On the other hand, for a reaction between two tethered molecules, the reaction rate is proportional to the effective concentration [? ? ?]. Effective concentration is defined as how often a ligand bound to the tail of one anchored polymer encounters a binding site on the tail of a second anchored polymer, taking into account the accessibility of the binding site. We will explore how effective concentration is impacted by ligand size and polymer length. We will generate plots of the effective concentration as function of separation distance in both free-space and half-space for multiple sizes of polymer and bound ligand. We expect these to look similar to the schematic shown in Fig. 6. Under simplified circumstances, e.g. no bound ligand, it has been shown that the effective concentration will be a half-gaussian [?]. Therefore, we expect our plots to also resemble a half-gaussian. We will fit a half-gaussian to these curves and consider the change in maximum effective concentration and width of the curve (reach parameter) between free-space and half-space.

We have shown that a polymer in half-space will have a mildly extended end-to-end distribution compared to a polymer in free-space (Fig. ??). For this reason, we expect only a mild change in the reach parameter between free-space and half-space.

It is less clear what effect a surface will have on maximum concentration. On the one hand, a membrane will force both polymers to occupy the same half space, which should enhance the effective concentration. On the other hand, we have seen that presence of a membrane reduces the accessibility of a binding site, decreasing effective concentration. We expect that for a small enough ligand, the membrane will lead to a net enhancement. We will answer whether, for a ligand of typical size, the membrane creates a net enhancement or reduction of the effective concentration.

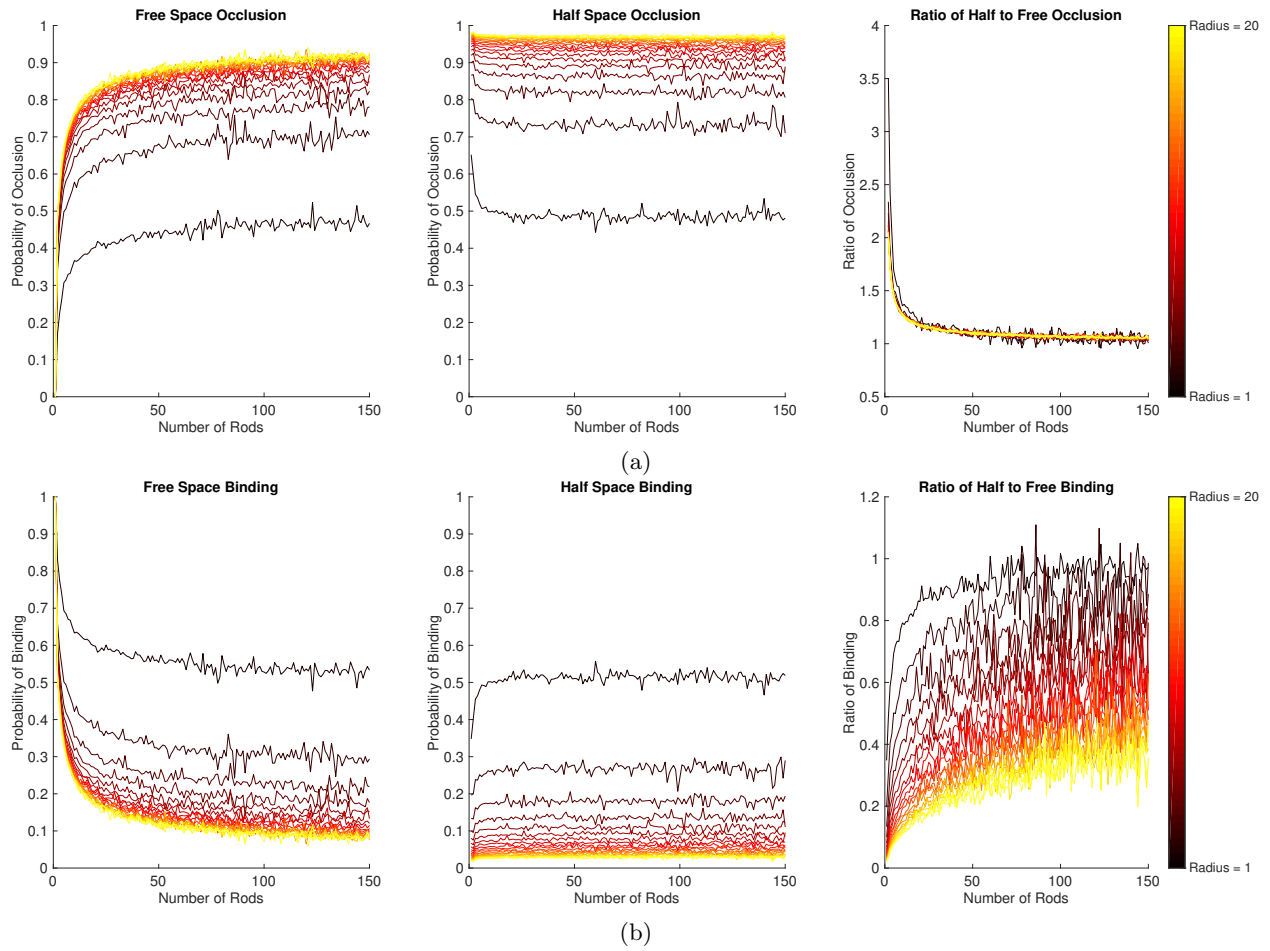


Figure 5: Probability of ligand being occluded,  $p_{occ}$  (top row), and probability of ligand binding,  $1 - p_{occ}$  (bottom row), as a function of tether length for various ligand radii. Free-space (left column), half-space (middle), and the ratio of probabilities half-space to free-space (right).

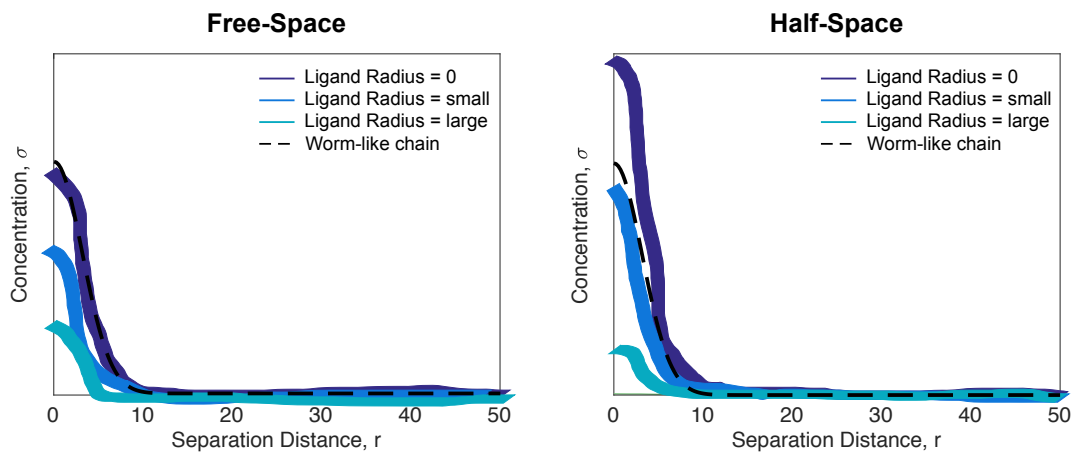


Figure 6: Possible plot of effective concentration as a function of tether separation distance.

### 1.3.3 Future Work: Experimental comparison of matrix-bound versus surface-bound tethered reactions

We compare the results from our simulations to preliminary data collected by our collaborators. The data represents the output of surface plasmon resonance experiments conducted with SHP-1 attached to three different tethers (PD1, PEG3, PEG28) on a matrix (CM5) and a surface (C1). We found that the presence of a surface will decrease the accessibility of the binding site. This change will cause an increase in the dissociation constant,  $K_D$ . Consistent with our simulated results, the  $K_D$  increases when the experiment is conducted on a surface compared to on a matrix for each tether (Fig. 7, 8, 9).

We will also compare our simulated changes in effective concentration to data. The change in effective concentration will manifest as a change in the observed catalytic rate,  $k_{cat}$ . If we establish a relation between the observed catalytic rate on a surface compared to a matrix, we can recalculate the experimental reach parameter to check for agreement. For example, in the shown data, we assume the observed  $k_{cat}$  on a surface is 1.2 fold increased over a matrix (red bar in Fig. 7, 8, 9). From this, we can recalculate the reach parameter to compare with simulated results.

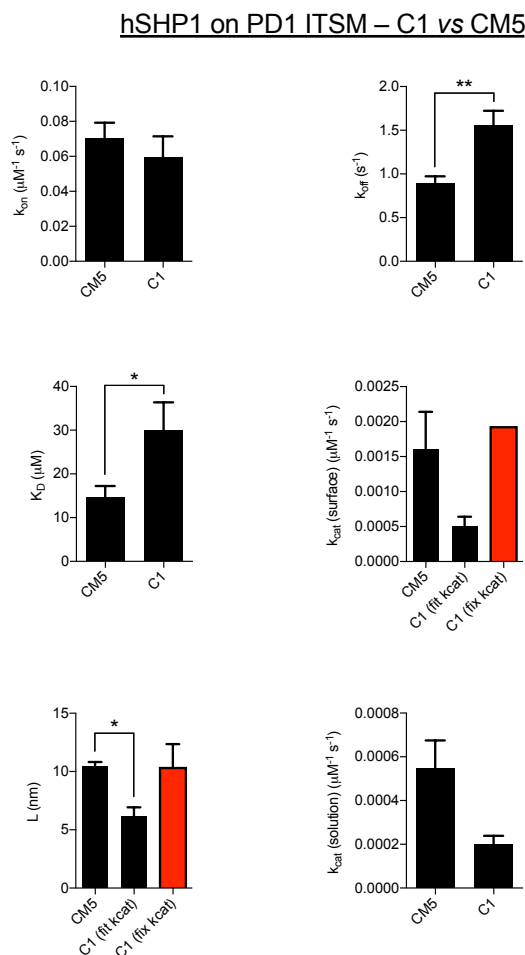


Figure 7: Preliminary comparison of tethered reaction of human SHP-1 dephosphorylating ITSM on PD1 performed on matrix (CM5) and surface (C1). Comparisons between (a) binding rate,  $k_{on}$  (b) unbinding rate,  $k_{off}$  (c) dissociation constant,  $K_D$  (d) catalytic rate tethered,  $k_{cat}(\text{surface})$  (e) reach parameter,  $L$ , (f) catalytic rate in solution,  $k_{cat}(\text{solution})$ . Change in reach parameter is also calculated under assumption that  $k_{cat}(\text{surface})$  on a surface is 1.2 fold increased over a matrix (red).

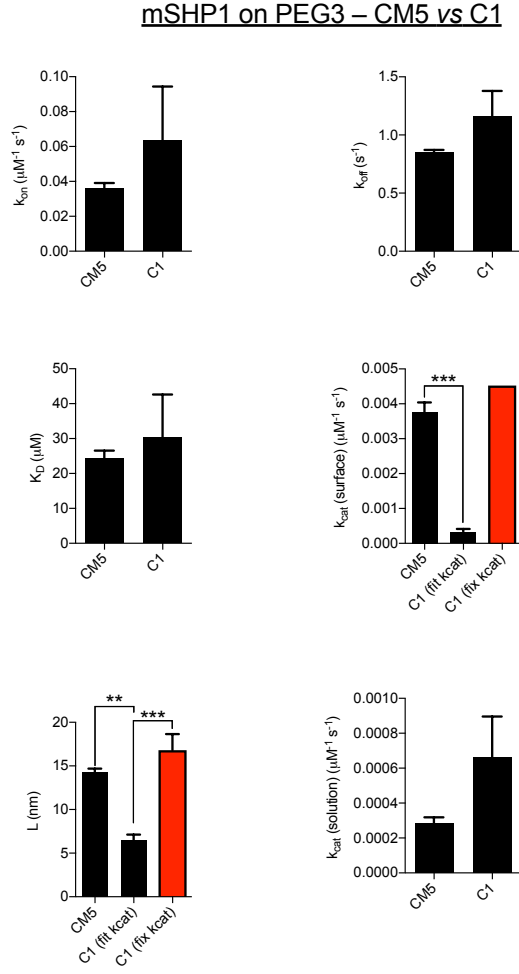


Figure 8: Preliminary comparison of tethered reaction of mouse SHP-1 dephosphorylating ITIM on PEG3 performed on matrix (CM5) and surface (C1) assuming tether reach unchanged. Comparisons between (a) binding rate,  $k_{on}$  (b) unbinding rate,  $k_{off}$  (c) dissociation constant,  $K_D$  (d) catalytic rate tethered,  $k_{cat}(\text{surface})$  (e) reach parameter,  $L$ , (f) catalytic rate in solution,  $k_{cat}(\text{solution})$ .



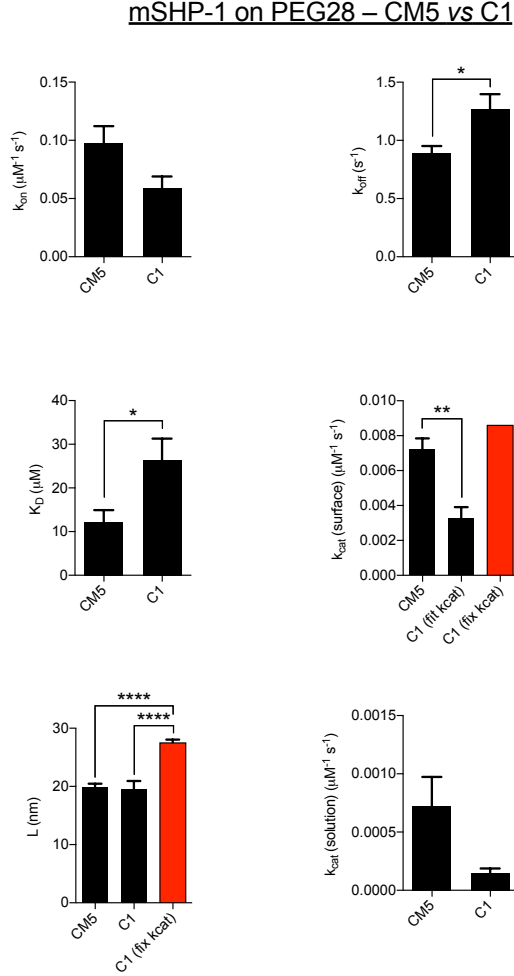


Figure 9: Preliminary comparison of tethered reaction of mouse SHP-1 dephosphorylating ITIM on PEG28 performed on matrix (CM5) and surface (C1) assuming tether reach unchanged. Comparisons between (a) binding rate,  $k_{on}$  (b) unbinding rate,  $k_{off}$  (c) dissociation constant,  $K_D$  (d) catalytic rate tethered,  $k_{cat}(\text{surface})$  (e) reach parameter,  $L$ , (f) catalytic rate in solution,  $k_{cat}(\text{solution})$ .

#### 1.3.4 Future Work: Catalysis surface factor versus contour length and versus ligand radius

Experimental measurements of effective concentration do not distinguish between the effective concentration and the catalytic rate. Since these values are lumped into a single number, it is important to know how the surface impacts the apparent catalytic rate. We will plot the ratio of apparent catalytic rates for various polymer lengths and ligand sizes. This will indicate if there is a relationship between the catalysis factor and the reaction parameters or if there is a single value describing the impact of the surface. The catalysis surface factor may then be used to determine how experiments on a surface differ from on a matrix and possibly give a conversion factor between the two.